



## METABOLIC, ENDOCRINE, AND GENITOURINARY PATHOBIOLOGY

# Vaginal Squamous Cell Carcinoma Develops in Mice with Conditional *Arid1a* Loss and Gain of Oncogenic *Kras* Driven by Progesterone Receptor Cre



Xiyin Wang,<sup>\*</sup> Mariana S.L. Praça,<sup>\*</sup> Jillian R.H. Wendel,<sup>\*</sup> Robert E. Emerson,<sup>†</sup> Francesco J. DeMayo,<sup>‡</sup> John P. Lydon,<sup>§</sup> and Shannon M. Hawkins<sup>\*</sup>

From the Department of Obstetrics and Gynecology,<sup>\*</sup> Indiana University School of Medicine, Indianapolis, Indiana; the Department of Pathology and Laboratory Medicine,<sup>†</sup> Indiana University School of Medicine, Indianapolis, Indiana; the National Institute of Environmental Health Sciences,<sup>‡</sup> Research Triangle Park, North Carolina; and the Department of Molecular and Cellular Biology,<sup>§</sup> Baylor College of Medicine, Houston, Texas

Accepted for publication  
March 19, 2021.

Address correspondence to  
Shannon M. Hawkins, M.D.,  
Ph.D., Indiana University School  
of Medicine, 550 N. University  
Blvd, UH2440, Indianapolis, IN  
46202. E-mail: [shhawkin@iu.edu](mailto:shhawkin@iu.edu).

Oncogenic KRAS mutations are a common finding in endometrial cancers. Recent sequencing studies indicate that loss-of-function mutations in the *ARID1A* gene are enriched in gynecologic malignant tumors. However, neither of these genetic insults alone are sufficient to develop gynecologic cancer. To determine the role of the combined effects of deletion of *Arid1a* and oncogenic *Kras*, *Arid1a*<sup>flox/flox</sup> mice were crossed with *Kras*<sup>Lox-Stop-Lox-G12D/+</sup> mice using progesterone receptor Cre (*Pgr*<sup>Cre/+</sup>). Histologic analysis and immunohistochemistry of survival studies were used to characterize the mutant mouse phenotype. Hormone dependence was evaluated by ovarian hormone depletion and estradiol replacement. *Arid1a*<sup>flox/flox</sup>; *Kras*<sup>Lox-Stop-Lox-G12D/+</sup>; *Pgr*<sup>Cre/+</sup> mice were euthanized early because of invasive vaginal squamous cell carcinoma. Younger mice had precancerous intraepithelial lesions. Immunohistochemistry supported the pathological diagnosis with abnormal expression and localization of cytokeratin 5, tumor protein P63, cyclin-dependent kinase inhibitor 2A, and Ki-67, the marker of proliferation. Ovarian hormone deletion in *Arid1a*<sup>flox/flox</sup>; *Kras*<sup>Lox-Stop-Lox-G12D/+</sup>; *Pgr*<sup>Cre/+</sup> mice resulted in atrophic vaginal epithelium without evidence of vaginal tumors. Estradiol replacement in ovarian hormone-depleted *Arid1a*<sup>flox/flox</sup>; *Kras*<sup>Lox-Stop-Lox-G12D/+</sup>; *Pgr*<sup>Cre/+</sup> mice resulted in lesions that resembled the squamous cell carcinoma in intact mice. Therefore, this mouse can be used to study the transition from benign precursor lesions into invasive vaginal human papillomavirus-independent squamous cell carcinoma, offering insights into progression and pathogenesis of this rare disease. (*Am J Pathol* 2021, 191: 1281–1291; <https://doi.org/10.1016/j.ajpath.2021.03.013>)

Recent sequencing studies, including The Cancer Genome Atlas (TCGA), PanCancer, and Memorial Sloan-Kettering Integrated Mutation Profiling and Actionable Cancer Targets (MSK-IMPACT), have highlighted potentially impactful mutations across gynecologic cancers.<sup>1,2</sup> Worldwide in 2020, nearly 1.4 million women were diagnosed with gynecologic cancer, and >672,000 women with gynecologic cancer died,<sup>3</sup> up from 528,000 deaths in 2018.<sup>4</sup> In silico analyses of multiple, large, publicly available datasets have found that a small subset of genes are mutated across uterine cervix, uterine corpus, ovary, vulval, or vaginal cancers.<sup>5</sup> However, the functional role of each of these genes in female reproductive tract

Supported by the Eunice Kennedy Shriver National Institute of Child Health and Human Development (NICHD) grant R24 HD102061 (The University of Virginia Center for Research in Reproduction Ligand Assay and Analysis Core), The Liz Tilberis Scholarship Ovarian Cancer Research Fund through the Estate of Agatha Fort (S.M.H.), grant 1R03 CA19127 A1 (S.M.H.), NIH/NICHD grant RO1 HD042311 (J.P.L.), and Coordenação de Aperfeiçoamento de Pessoal de Nível Superior (M.S.L.P.). Dr. DeMayo was supported by the Intramural Research Program of the National Institute of Environmental Health Sciences project Z1AES103311-01.

X.W. and M.S.L.P. contributed equally to this work.

Current address of X.W., Graduate School of Biomedical Sciences, Mayo Clinic, Rochester, MN; of M.S.L.P., Department of Obstetrics and Gynecology, Federal University of Minas Gerais and Group of Health, Mater Dei, Belo Horizonte — MG, Brazil.

malignant tumors remains mostly unknown. Models of these diseases have the potential to improve the understanding of disease pathogenesis, accelerate the discovery of novel therapeutics, and improve the lives of many women worldwide.

AT-rich interactive domain 1A (ARID1A) is one of eight genes whose mutation frequency is significantly higher in gynecologic malignant tumors over other cancers.<sup>5</sup> Loss-of-function mutations in *ARID1A* are frequent in endometriosis-associated ovarian cancers, endometrial cancers, and cervical cancers.<sup>1,2,5–12</sup> More than 40% of endometrial cancers have a mutation in *ARID1A*.<sup>8–10</sup> Of human papillomavirus (HPV)–negative cervical squamous cell carcinomas, 33% contained mutations in *ARID1A*.<sup>12</sup> *ARID1A* encodes a protein in the switch/sucrose nonfermentable chromatin remodeling complex, playing a role in transcriptional regulation and reprogramming.<sup>10,13,14</sup> The ARID1A protein plays an essential role in female reproduction and is ubiquitously expressed in the female reproductive tract.<sup>15,16</sup> Conditional deletion of *Arid1a* with the antimüllerian hormone receptor 2 *Cre* resulted in subfertility because of abnormal placentation.<sup>15</sup> Conditional deletion of *Arid1a* with the progesterone receptor *Cre* (*Pgr<sup>Cre/+</sup>*) or the lactotransferrin *Cre* resulted in infertility because of endometrial dysfunction.<sup>16,17</sup> Deletion of *Arid1a* alone in the mouse female reproductive tract was not sufficient to drive cancer.<sup>13–18</sup> Additional gene deletions were required for the development of gynecologic malignant tumors.<sup>13,14,18–22</sup>

Mutations in *KRAS* are frequent in gynecologic malignant tumors. *KRAS* is mutated in >10% of samples across multiple large datasets.<sup>5</sup> Oncogenic *KRAS* has been detected in up to 30% of endometrial cancers.<sup>23–25</sup> Increased expression of *KRAS* is associated with low overall survival across gynecologic cancers.<sup>5</sup> Conditional expression of *Kras<sup>G12D</sup>* alone was insufficient to develop cancer in mice.<sup>26–29</sup> However, *Pten* conditional deletion in *Kras<sup>G12D</sup>*-expressing mice was sufficient for gynecologic malignant tumors.<sup>27–31</sup> Similar to deletion of *Arid1a* alone, the gain of oncogenic *Kras<sup>G12D</sup>* alone in the female reproductive tract was not sufficient to drive cancer,<sup>26,28,29,32</sup> and additional gene deletions were required in genetically engineered mouse models.<sup>19,26–29,31,33–35</sup>

In humans, concurrent mutations in *ARID1A* and *KRAS* are frequent in mesonephric-like müllerian adenocarcinomas of the female reproductive tract.<sup>36</sup> Similarly, simultaneous mutations are common in endometrial and cervical cancer and are rare, yet present, in ovarian cancer.<sup>1,2,5,8,12,37,38</sup> These previous results in humans led to the hypothesis that conditional *Arid1a* deletion in *Kras<sup>G12D</sup>*-expressing mice using *Pgr<sup>Cre</sup>* would generate female reproductive tract cancer.

## Materials and Methods

### Animal Husbandry and Genotyping

Animal experiments were approved by the Indiana University School of Medicine Institutional Animal Care and Use Committee (Indianapolis, IN). Animals were handled according to

the NIH's *Guide for the Care and Use of Laboratory Animals*.<sup>39</sup> All mice were bred and kept under standard conditions. *Arid1a<sup>flox/flox</sup>*; *Pgr<sup>Cre/+</sup>* mice<sup>16</sup> and *Kras<sup>Lox-Stop-Lox-G12D/+</sup>* mice<sup>28</sup> or *Pgr<sup>Cre/+</sup>* mice<sup>40</sup> and *Kras<sup>Lox-Stop-Lox-G12D/+</sup>* mice<sup>28</sup> were crossbred and maintained on a C57BL/6J; 129S5/Brd mixed hybrid background to generate *Arid1a<sup>flox/flox</sup>*; *Kras<sup>Lox-Stop-Lox-G12D/+</sup>*; *Pgr<sup>Cre/+</sup>* (AKP), *Kras<sup>Lox-Stop-Lox-G12D/+</sup>*; *Pgr<sup>Cre/+</sup>* (KP), and *Pgr<sup>+/+</sup>* (control) mice (Supplemental Figure S1). Mice were genotyped at 12 to 14 days of postnatal life from tail biopsy specimens by PCR as previously described.<sup>15,41,42</sup> *Cre*-mediated recombination in *Arid1a<sup>flox/flox</sup>* mice removes exon 8, leading to loss of protein.<sup>43</sup> *Cre*-mediated recombination of *Kras<sup>Lox-Stop-Lox-G12D/+</sup>* mice removes the stop codon, resulting in the expression of oncogenic *Kras<sup>G12D</sup>*.<sup>44</sup> *Pgr<sup>Cre/+</sup>* drives *Cre*-mediated recombination where progesterone receptor is expressed.<sup>40</sup> For survival studies, mice were caged, examined twice weekly, and euthanized at humane endpoints.<sup>42</sup> Postmortem tail clips were used to confirm genotyping,<sup>15,41,42</sup> and mice with inconsistent genotypes were reassigned or removed.

### Histologic Analyses

Tissues were fixed, stained, and quantified as previously described.<sup>42</sup> The Lower Anogenital Squamous Terminology project nomenclature was used to describe histologic findings.<sup>45</sup> All histologic findings were interpreted by a surgical pathologist (R.E.E.). Antibodies for immunohistochemistry are listed in Table 1. Immunohistochemistry and immunofluorescence were performed as previously described,<sup>42</sup> confirming deletion of ARID1A and expression of *KRAS* proto-oncogene, GTPase (*KRAS<sup>G12D</sup>*) in AKP uterine and vaginal tissues (Supplemental Figure S2).

### Serum Analysis

Mice were anesthetized by isoflurane (Abbott Laboratories, North Chicago, IL), and blood was collected in microtainer tubes (Becton Dickinson, Franklin Lakes, NJ) by closed cardiac puncture. The serum was separated by centrifugation and stored at  $-20^{\circ}\text{C}$  until use. The University of Virginia Ligand Assay and Analysis Core performed measurements of follicle-stimulating hormone and luteinizing hormone by radioimmunoassay.

### Steroid Hormone Treatment

Mice underwent ovariectomy at 6 weeks. Mice were randomly divided into treatment groups: estradiol pellet (0.25 mg of 17- $\beta$ -estradiol per 60-day release pellet; Innovative Research of America, Sarasota, FL) or no pellet (sham) and tissues collected after 60 days.

**Table 1** Antibodies Used for Immunostaining

Antibody name	Company	Catalog number	Dilution
ARID1A	Santa Cruz Biotechnology (Dallas, TX)	sc-98441	1:100
KRAS <sup>G12D</sup>	Abcam (Cambridge, UK)	Ab221163	1:20
CK5	Cell Signaling Technology (Danvers, MA)	71536S	1:50
p63	Genetex (Irvine, CA)	GTX102425	1:100
p16	Abcam	Ab108349	1:100
Anti-Ki-67	MilliporeSigma (Burlington, MA)	AB9260	1:300
Goat anti-rabbit IgG	Vector Laboratories (Burlington, MA)	BA-1000	1:200

ARID1A, AT-rich interactive domain 1A; CK5, cytokeratin 5; KRAS<sup>G12D</sup>, KRAS proto-oncogene, GTPase; p16, cyclin-dependent kinase inhibitor 2A; p63, tumor protein P63.

## Statistical Analysis

Log-rank (Mantel-Cox) test, Fisher's exact test, *t*-test, and multiple *t*-tests were performed using the InStat package for GraphPad Prism version 8 (GraphPad, San Diego, CA). *P* < 0.05 was considered statistically significant.

## Results

### Large Vaginal Tumors

As per the criteria for humane endpoints,<sup>42</sup> AKP mice had decreased survival compared with *Pgr*<sup>+/+</sup> mice (Figure 1A and Supplemental Figure S3). The median survival of AKP mice was 106 days. AKP mice (10 of 10) exhibited gross,

solid lesions protruding from the vagina, resulting in early euthanasia. These lesions were pink-red, with oblong to round growth on the outer part of the vagina (Figure 1B). On dissection, the gross lesions appeared to be confined to the vagina, with grossly normal ovaries, oviducts, and uterus (Figure 1C).

*Pgr*<sup>+/+</sup> female mice had normal-appearing vaginal histologic findings with well-defined epithelial layers, including a keratinized outer layer of cells without nuclei, stratified squamous epithelium, and lamina propria (Figure 1D). AKP mice had squamous cell carcinoma with central keratinization surrounded by highly dysplastic squamous epithelium as evidenced by the large, dark nuclei and disorganized cellular pattern, along with nests of cells with abundant eosinophilic cytoplasm (Figure 1E).

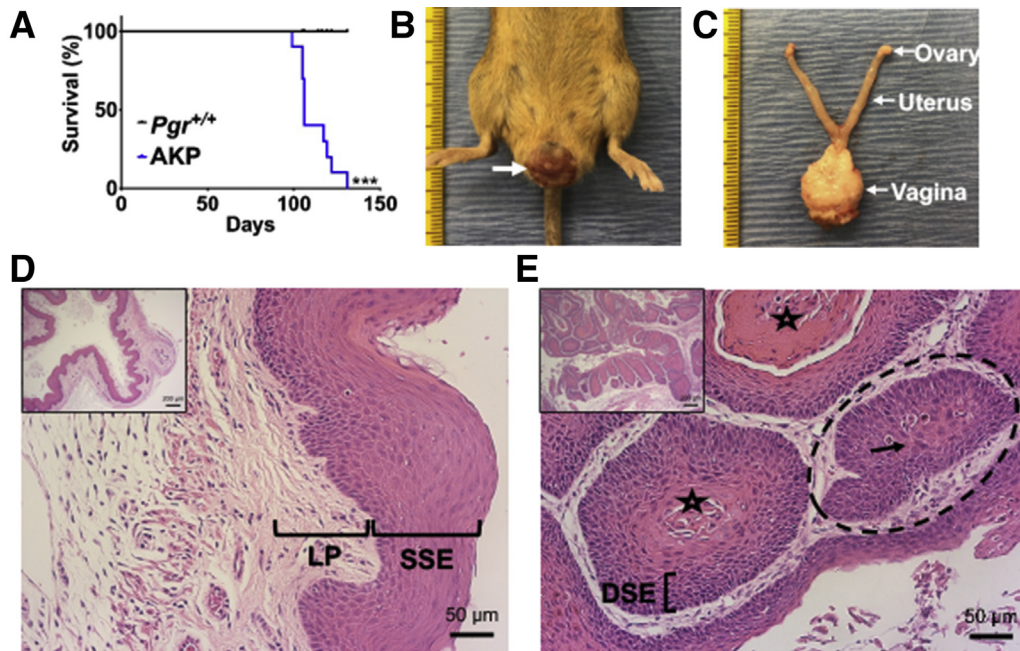


**Figure 1** Poor survival and squamous cell carcinoma in *Arid1a*<sup>flox/flox</sup>; *Kras*<sup>Lox-Stop-Lox-G12D/+</sup>; *Pgr*<sup>Cre/+</sup> (AKP) female mice. **A:** Kaplan-Meier survival curves were analyzed by the log-rank (Mantel-Cox) test. AKP mice had decreased survival compared with control mice. **B:** Gross vaginal tumor burden (white arrow) in AKP mice. **C:** Gross lesions were localized to the vagina with grossly normal ovaries, oviducts, uterus, and cervix. Tick marks on ruler indicate 1 mm. **D:** Control vagina had normal keratinized stratified squamous epithelium (SSE) and lamina propria (LP). **E:** AKP vagina exhibited squamous cell carcinoma lined by highly dysplastic squamous epithelium (DSE) with central keratinization (star) and nests of cells (dashed circle) with abundant eosinophilic cytoplasm (black arrow). Hematoxylin and eosin staining. *n* = 10 per group (A). \*\*\**P* < 0.001. Scale bars: 50  $\mu$ m (D and E, main images); 200  $\mu$ m (D and E, insets).



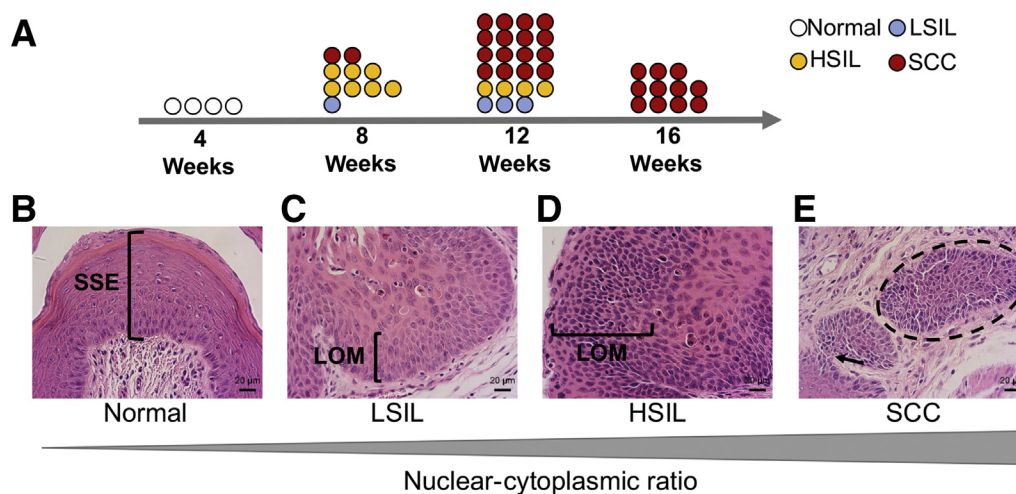


**Figure 2** Squamous intraepithelial lesions and squamous cell carcinoma in *Arid1a*<sup>flox/flox</sup>; *Kras*<sup>Lox-Stop-Lox-G12D/+</sup>; *Pgr*<sup>Cre/+</sup> (AKP) mice. **A:** Schematic timeline of the progression of squamous intraepithelial lesions to squamous cell carcinoma in AKP mice. **B:** At 8 weeks, *Pgr*<sup>+/+</sup> vagina had normal stratified squamous epithelium (SSE). **C:** Ten percent of AKP vaginas contained low-grade squamous intraepithelial lesions (LSILs) with increased nuclear/cytoplasmic ratios and loss of maturation (LOM) in the lower epithelium. **D:** Seventy percent of AKP vaginas exhibited high-grade squamous intraepithelial lesions (HSILs) with cell crowding, high nuclear/cytoplasmic ratio, and LOM in at least two-thirds of the epithelium. **E:** Twenty percent of AKP vaginas had squamous cell carcinoma with nests of cells (dashed circle) and highly dysplastic squamous epithelium invading through the stroma (black arrow). Hematoxylin and eosin staining. Scale bar = 20  $\mu$ m.

Additional examples of squamous cell carcinoma are in [Supplemental Figure S4](#), and individual mouse female reproductive tract histologic findings are listed in [Supplemental Table S1](#).

### Early Precancerous Lesions Leading to Cancer

In women, invasive squamous cell carcinoma develops from precancerous lesions, including low-grade squamous intraepithelial lesions (LSILs, also known as vaginal intraepithelial neoplasia 1) or high-grade squamous intraepithelial lesions (HSILs, vaginal intraepithelial neoplasia 2 and 3).<sup>46</sup> As AKP mice aged, the penetrance of squamous cell carcinoma increased ([Figure 2A](#)). Squamous intraepithelial lesions were not found in *Pgr*<sup>+/+</sup> mice ([Figure 2B](#)). As early as 8 weeks, 10% (1 of 10) of AKP mice exhibited LSILs. The nuclei in the epithelium were enlarged with variable size, irregular nuclear contours, and increased nuclear/cytoplasmic ratios ([Figure 2C](#)). Most frequently (7 of 10), AKP mice at 8 weeks had HSILs. The epithelium exhibited a full-thickness proliferation of abnormal parabasal-like cells with loss of maturation and increased nuclear/cytoplasmic ratios ([Figure 2D](#)). As early as 8 weeks, AKP mice (2 of 10) had invasive squamous cell carcinoma ([Figure 2E](#)). Additional magnification views are in [Supplemental Figure S5](#). By 12 weeks, nearly 70% (16 of 23) of AKP mice developed squamous cell carcinoma ([Figure 2A](#) and [Supplemental Table S2](#)). At 16 weeks, 100% (11 of 11) AKP mice exhibited squamous cell carcinoma ([Figure 2A](#) and [Supplemental Table S2](#)).

Because previous studies examined the 2-month time point for KP mice,<sup>29</sup> KP mice were examined for

precancerous lesion development. At 8 weeks, only one of six KP mice exhibited HSILs ([Supplemental Figure S6](#) and [Supplemental Table S3](#)). The frequency of abnormal squamous histologic findings was higher in AKP mice than in KP mice at 8 weeks (Fisher's exact test = 0.0014,  $P < 0.01$ ).

### Atypical Lesions Outside the Vagina

*Pgr*<sup>Cre/+</sup> results in *Cre*-mediated recombination in the uterus, oviduct, and ovaries.<sup>40</sup> However, no malignant tumors were identified in the AKP mice besides the vagina. AKP mice had normal ovaries, with normal follicular development ([Supplemental Figure S7](#)). Consistent with normal follicular steroid hormone feedback, no significant differences were observed between *Pgr*<sup>Cre/+</sup> and AKP mice in follicle-stimulating hormone levels (*Pgr*<sup>+/+</sup>:  $3.607 \pm 0.363$  ng/mL,  $n = 10$ ; AKP:  $4.952 \pm 1.857$  ng/mL,  $n = 10$ ; unpaired, two-tailed  $t$ -test,  $P = 0.487$ ) or luteinizing hormone levels (*Pgr*<sup>+/+</sup>:  $0.230 \pm 0.060$  ng/mL,  $n = 12$ ; AKP:  $0.200 \pm 0.031$  ng/mL,  $n = 10$ ; unpaired, two-tailed  $t$ -test,  $P = 0.666$ ).

In some cases (5 of 14 mice), the oviductal epithelium in AKP mice at 16 weeks contained atypical epithelium with nuclear stratification and multiple layers of epithelial cells with nuclear atypia in the form of nuclear enlargement and rounding ([Supplemental Figure S7](#) and [Supplemental Table S2](#)). There was no difference in body weight between AKP and *Pgr*<sup>+/+</sup> mice at any time point (data not shown). Uterine weight per body weight in AKP mice at 16 weeks was more than that in control mice (AKP:  $4.2 \pm 0.29$  mg/g; control:  $3.2 \pm 0.29$  mg/g; multiple  $t$ -test,  $P < 0.05$ ), but no

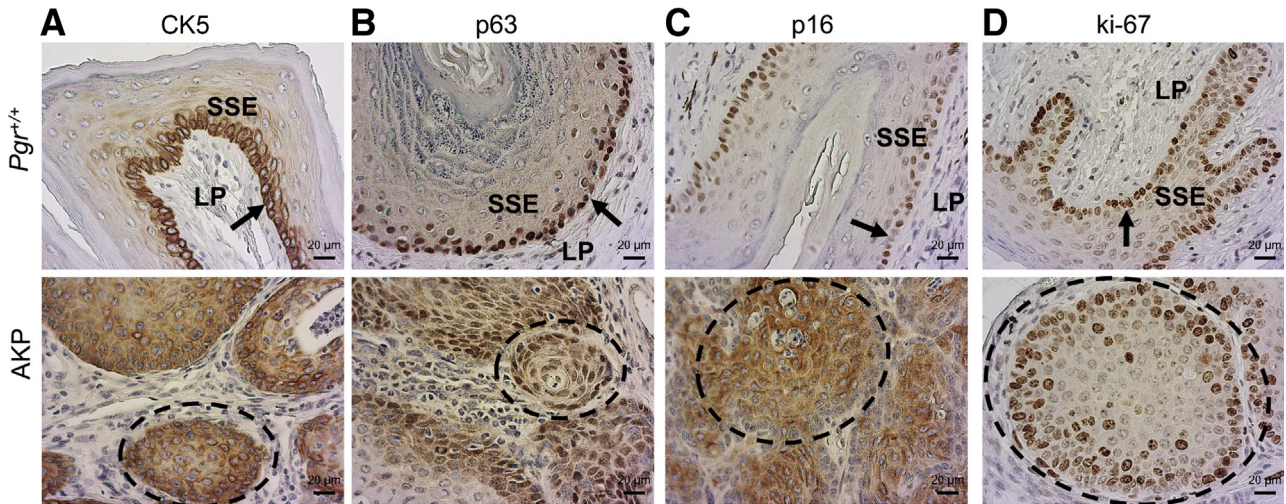


**Figure 3** A–D: Molecular immunohistochemical staining for cytokeratin 5 (CK5) (A), tumor protein P63 (p63) (B), cyclin-dependent kinase inhibitor 2A (p16) (C), and marker of proliferation Ki-67 (D). **Arrow** indicates basal layer; **dashed circle**, nests of squamous cell carcinoma. Scale bar = 20 μm. SSE, stratified squamous epithelium, LP, lamina propria.

significant difference was found in uterine weight at 12 weeks (AKP:  $3.5 \pm 0.25$  mg/g; *Pgr*<sup>+/+</sup>:  $3.4 \pm 0.35$  mg/g; multiple *t*-test,  $P = 0.88$ ) or at 8 weeks (AKP:  $2.9 \pm 0.16$  mg/g; *Pgr*<sup>+/+</sup>:  $3.5 \pm 0.69$  mg/g; multiple *t*-test,  $P = 0.28$ ). Endometrial hyperplasia was observed in 21% (3 of 11) AKP mice at 16 weeks with enlarged glands separated by minimal amounts of stroma (Supplemental Figure S8 and Supplemental Table S2). Nuclear atypia was also observed with loss of polarity and rounding of the nuclei (Supplemental Figure S8). Endometrial adenocarcinoma was not observed in AKP mice. Squamous cell carcinoma was not detected in the cervix of AKP mice (Supplemental Table S2).

### Molecular Characterization

Cytokeratin 5 (CK5) is a useful stain for squamous differentiation.<sup>46,47</sup> The basal epithelial cells of the *Pgr*<sup>+/+</sup> vagina showed intense perinuclear and moderate cytoplasmic CK5 expression with little to no staining in the lamina propria (Figure 3A and Supplemental Figure S9). Intense cytoplasmic and perinuclear CK5 staining was observed throughout the full thickness of the vaginal squamous cell carcinoma nests but sparing the underlying lamina propria (Figure 3A and Supplemental Figure S9). Intense nuclear staining for the basal epithelial cell marker tumor protein P63 (p63)<sup>48</sup> was demonstrated in the basal layer of the *Pgr*<sup>+/+</sup> vagina. Moderately intense nuclear p63 staining was observed across the full thickness of the nests of squamous cell carcinoma in AKP vaginas (Figure 3B and Supplemental Figure S9). Vaginal squamous cell carcinoma in women has diffuse staining for cyclin-dependent kinase inhibitor 2A (also known as p16).<sup>46,49</sup> The *Pgr*<sup>+/+</sup> vagina showed low-intensity, low-frequency nuclear staining for p16 which was limited to the basal layer. Nests of vaginal squamous cell carcinoma in AKP

mice had intense, diffusely positive p16 staining (Figure 3C and Supplemental Figure S9). Marker of proliferation, Ki-67, staining in *Pgr*<sup>+/+</sup> mice was contained to a mostly single layer of the basal epithelium of the vagina. Ki-67 staining in AKP mice was seen in multiple layers in the nests of squamous cell carcinoma (Figure 3D and Supplemental Figure S9).

### Hormone-Dependent and Estradiol-Responsive Tumors

Ovaries were removed at 6 weeks of age, and AKP and *Pgr*<sup>+/+</sup> mice were examined 6 weeks later (at 12 weeks of age). Ovarian hormone-depleted AKP and *Pgr*<sup>+/+</sup> mice at 12 weeks had zero gross lesions ( $n = 8$ ) (Supplemental Table S4), suggesting that AKP vaginal squamous cell carcinoma may be hormone dependent. To assess hormone responsiveness, ovariectomized AKP and ovariectomized *Pgr*<sup>+/+</sup> mice were treated with a 17-β-estradiol pellet or sham for 60 days. Both ovariectomized *Pgr*<sup>+/+</sup> sham and ovariectomized AKP sham mice had no gross vaginal or uterine lesions, and the uteri were of grossly smaller size than those of intact mice (ovariectomized *Pgr*<sup>+/+</sup> sham mice:  $0.51 \pm 0.06$  mg/g; *Pgr*<sup>+/+</sup> mice with intact ovaries:  $3.24 \pm 0.29$  mg/g; two-tailed *t*-test;  $P < 0.0001$ ; and ovariectomized AKP sham mice:  $0.48 \pm 0.054$  mg/g; AKP mice with intact ovaries:  $4.25 \pm 0.29$  mg/g; two-tailed *t*-test;  $P < 0.0001$ ) (Figure 4). Ovariectomized *Pgr*<sup>+/+</sup>-E2 uteri were translucent and cystically dilated, consistent with the edematous effects of estradiol in the uterus. Ovariectomized *Pgr*<sup>+/+</sup>-E2 mice had no gross vaginal lesions (Figure 4). Ovariectomized AKP-E2 uteri did not exhibit the characteristic cystic enlargement of estradiol treatment. Ovariectomized AKP-E2 uteri were larger than ovariectomized AKP-sham uteri (ovariectomized AKP-sham mice:  $0.48 \pm 0.054$  mg/g; ovariectomized AKP-E2 mice:  $24.6 \pm 15.2$  mg/g; two-tailed *t*-test;  $P < 0.0001$ ).



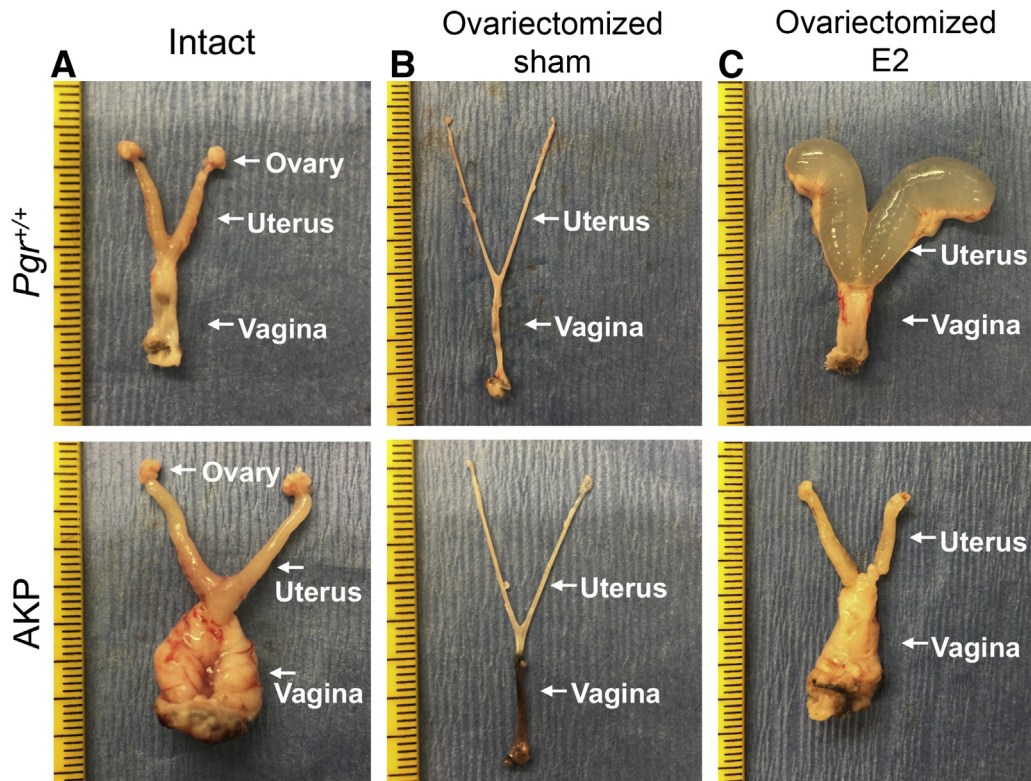


**Figure 4** Gross lesions in *Arid1a*<sup>flox/flox</sup>; *Kras*<sup>Lox-Stop-Lox-G12D/+</sup>; *Pgr*<sup>Cre/+</sup> (AKP) mice with 17- $\beta$ -estradiol treatment for 60 days. **A:** *Pgr*<sup>+/+</sup> intact mice were grossly normal. Intact AKP mice exhibited large gross vaginal lesions. **B:** Both ovariectomized *Pgr*<sup>+/+</sup> sham and ovariectomized AKP sham mice had tiny, thin uteri without gross vaginal lesions. **C:** Ovariectomized *Pgr*<sup>+/+</sup>-E2 mice had enlarged fluid-filled uteri. Ovariectomized AKP-E2 mice exhibited gross vaginal lesions but without the edematous cystic nature of the uterus. Tick marks on the ruler indicate 1 mm.

However, the ovariectomized AKP-E2 uteri were similar to AKP-intact uteri in that they appeared smooth and solid. Most ovariectomized AKP-E2 mice (4 of 6) exhibited exophytic gross vaginal lesions (Figure 4 and Supplemental Table S5).

Both ovariectomized *Pgr*<sup>+/+</sup>-sham and ovariectomized AKP-sham uteri were smaller than intact uteri (Supplemental Figure S10). Histologically, uteri from AKP intact mice had endometrial hyperplasia with an increased surface area of luminal epithelium, crowding of glandular epithelium, and little stroma between glands (Figure 5 and Supplemental Figure S10 and Supplemental Table S2). Neither ovariectomized *Pgr*<sup>+/+</sup>-sham nor ovariectomized AKP-sham mice had any evidence of endometrial hyperplasia. Both contained a single layer of benign luminal epithelium and the expected number of endometrial glands without evidence of atypia (Figure 5 and Supplemental Figure S10 and Supplemental Table S5).

Ovariectomized *Pgr*<sup>+/+</sup> mice treated with 17- $\beta$ -estradiol for 60 days (*Pgr*<sup>+/+</sup>-E2) had edematous, enlarged uteri. Clear fluid resulted in dilated lumina. The luminal epithelium existed in a single layer that maintained polarity without evidence of nuclear atypia (Figure 5 and Supplemental Figure S10). Ovariectomized AKP-E2 uteri were not dilated by fluid. Instead, they were lined mainly by epithelium with squamous metaplasia without evidence

of adenocarcinoma or nuclear atypia (Figure 5 and Supplemental Figure S10). Other nonmalignant phenotypes included endometrial hyperplasia (1 of 6 mice) and stump pyometra (2 of 6 mice) (Supplemental Table S5). The hyperplasia and metaplasia seen in ovariectomized AKP-E2 mice (4 of 6) was more penetrant than the hyperplasia observed in 16-week-old mice with intact ovaries (3 of 11).

The vaginal tissue was also hormone responsive. Histologically, hormone depletion in *Pgr*<sup>+/+</sup> vaginas (in ovariectomized *Pgr*<sup>+/+</sup>-sham mice) resulted in a thin single epithelial layer, with decreased keratinization (Figure 6 and Supplemental Figure S11), consistent with models of vaginal atrophy in rodents.<sup>50</sup> Treatment with 17- $\beta$ -estradiol pellets for 60 days (ovariectomized *Pgr*<sup>+/+</sup>-E2 mice) reversed these effects, a finding similar to that of previous studies.<sup>50</sup> Ovariectomized *Pgr*<sup>+/+</sup>-E2 vaginas exhibited normal keratinized stratified squamous epithelium and normal lamina propria (Figure 6 and Supplemental Figure S11). Similarly, ovariectomized AKP-sham vaginas revealed a thin layer of vaginal epithelium in more than a single layer. Treatment with estradiol reversed the benign, atrophic vaginal histologic findings in the ovariectomized AKP vaginas to squamous cell carcinoma (Figure 6 and Supplemental Figure S11). Histologic descriptions of each animal can be found in Supplemental Table S5.

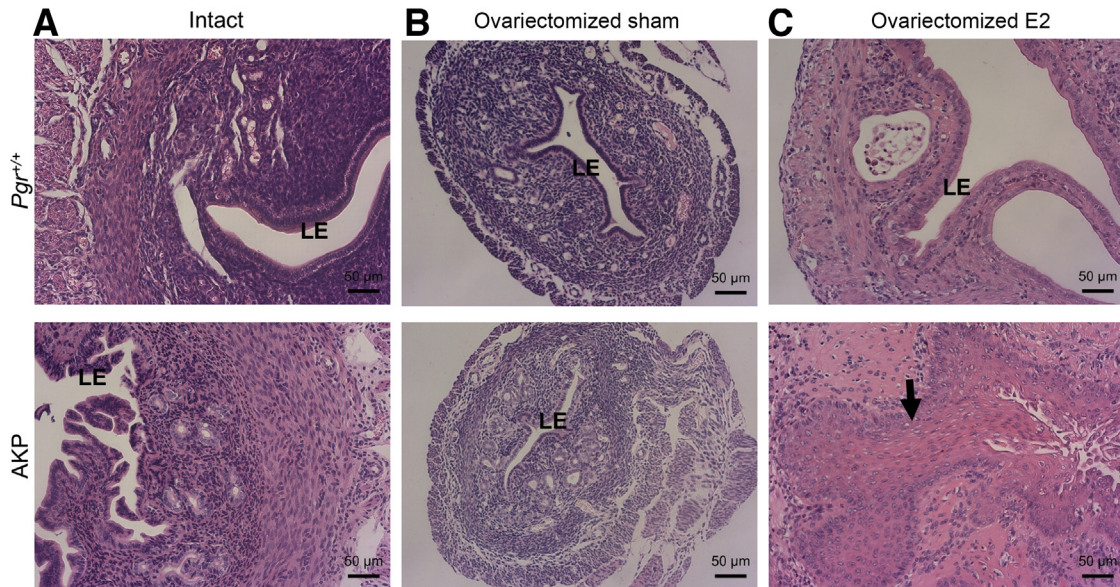


**Figure 5** Uterine histologic analysis in *Pgr*<sup>+/+</sup> and *Arid1a*<sup>flox/flox</sup>; *Kras*<sup>Lox-Stop-Lox-G12D/+</sup>; *Pgr*<sup>Cre/+</sup> (AKP) mice with and without 17- $\beta$ -estradiol (E2) treatment. **A:** 16-week-old intact *Pgr*<sup>+/+</sup> and AKP mouse uteri are shown for comparison. **B:** AKP intact uteri have endometrial hyperplasia. Ovariectomized AKP sham mice are similar in histologic findings to ovariectomized *Pgr*<sup>+/+</sup> sham mice. **C:** Ovariectomized *Pgr*<sup>+/+</sup>-E2 mice had enlarge dilated uteri without evidence of endometrial hyperplasia or atypia. Ovariectomized AKP-E2 mice had squamous metaplasia of the endometrium (**black arrow**). Hematoxylin and eosin staining. Scale bar = 50  $\mu$ m. LE, luminal epithelium.

## Concurrent Mutations in Human Squamous Cells Lower Female Reproductive Tract Cancers

To examine the co-occurrence of mutations in *ARID1A* and *KRAS* in human cancer datasets, in silico analysis of existing datasets was performed. Vaginal squamous cell carcinoma was not selected for large-scale genomic sequencing by TCGA. Examination of the MSK-IMPACT Clinical Sequencing Cohort ( $n = 10,945$ ) found that *ARID1A* and *KRAS* mutations tended to co-occur ( $P < 0.001$ ) across all cancer types.<sup>1</sup> However, only 50 of the MSK-IMPACT Clinical Sequencing Cohort were cervical cancer samples, and none were vaginal or vulvar cancer samples.<sup>1</sup> Cervical cancer subset from the TCGA PanCancer dataset, containing 278 samples,<sup>2</sup> had *ARID1A* (20 of 278 or 7.2%) and *KRAS* (16 of 278 or 5.8%) mutations. Concurrent mutations in both *ARID1A* and *KRAS* were present (2 of 278 or <1%) with a co-occurrence tendency ( $P = 0.322$ ). Limiting the dataset to 251 samples derived from cervical squamous cell carcinoma revealed 11 samples with mutations in *ARID1A* (11 of 251 or 4.4%). Of those 11 samples, two also had mutations in *KRAS* (2 of 11 or 18.2%). Both cervical squamous cell carcinoma samples with *ARID1A* and *KRAS* mutations were HPV negative.

## Discussion

A small subset of mutated genes is enriched in female reproductive tract malignant tumors,<sup>5</sup> with unclear

functional role. The AKP mouse was created to study two such genes. In the current study, AKP mice developed highly penetrant, hormone-responsive squamous cell carcinoma in the vagina. Of note, the vaginal squamous cell carcinoma described here is HPV independent. In support of the translational implications of this combination of genetic changes, in silico analysis of large-scale genome sequencing studies indicated the presence of concurrent mutations in *ARID1A* and *KRAS* in HPV-negative squamous cell cervical carcinoma samples, the closest genome-wide sequencing dataset to vaginal squamous cell carcinoma. Therefore, this model potentially represents a unique HPV-negative molecular subset of vaginal squamous cell carcinoma.

Because the *Pgr*<sup>Cre</sup> mouse is a powerful *Cre* recombinase for endometrial cancer modeling,<sup>51</sup> our original hypothesis was that AKP female mice would develop endometrial cancer. Oncogenic *KRAS* has been detected in up to 30% of endometrial cancers from women.<sup>23–25</sup> More than 40% of endometrial cancers from women have a mutation in *ARID1A*.<sup>8–10</sup> Loss of a proposed tumor suppressor and gain of an oncogene in the uterus leads to endometrial cancer.<sup>13,15–17</sup> There are a number of reasons why these mice did not develop endometrial cancer. First, the mice with aggressive early vaginal tumors were euthanized early for humane reasons. By 16 weeks, AKP mice had large, aggressive vaginal tumors, limiting the ability to study other gynecologic malignant tumors that may develop at older time points. Second, the molecular effects of *ARID1A* and *KRAS* in the vagina versus the uterus may be tissue-specific. The fact that neither deletion of *Arid1a* nor expression of oncogenic *Kras* alone is sufficient to drive cancer even with



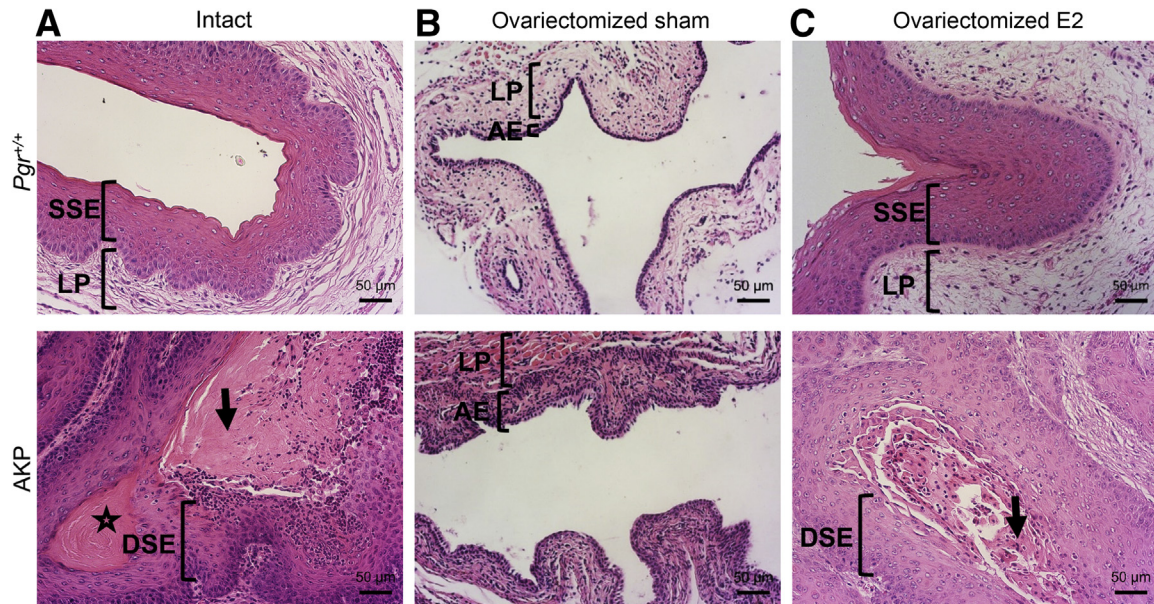


**Figure 6** Vaginal histologic analysis in *Pgr*<sup>+/+</sup> and *Arid1a*<sup>flox/flox</sup>; *Kras*<sup>Lox-Stop-Lox-G12D/+</sup>; *Pgr*<sup>Cre/+</sup> (AKP) mice with and without 17- $\beta$ -estradiol (E2) treatment. **A:** 16-week-old intact *Pgr*<sup>+/+</sup> and AKP mouse vaginas are shown for comparison. **B:** Intact *Pgr*<sup>+/+</sup> vaginas exhibited normal keratinized stratified squamous epithelium (SSE) with underlying lamina propria (LP). Intact AKP vaginas showed squamous cell carcinoma with central keratinization (**star**), eosinophilic cytoplasm (**arrow**), and dysplastic squamous epithelium (DSE). Ovariectomized *Pgr*<sup>+/+</sup> sham vaginas had signs of vaginal atrophy with thin atrophic epithelium (AE) and thin lamina propria. **C:** Hormone replacement resulted in a thickened epithelial layer with keratinization and normal lamina propria. **B:** Ovariectomized AKP sham mice had thinning of vaginal epithelium without evidence of carcinoma. **C:** Ovariectomized AKP-E2 mice exhibited squamous cell carcinoma with dysplastic squamous epithelium (DSE) and eosinophilic cytoplasm (**black arrow**). Hematoxylin and eosin staining. Scale bar = 50  $\mu$ m.

multiple different *Cre* recombinases<sup>13–18,26,28,29,32</sup> supports the idea of dual genetic contributions being important in malignant transformation.

The AKP mouse described here has unique caveats compared with other mouse models with *Arid1a*<sup>flox</sup> allele. First, the *Arid1a*<sup>flox</sup> allele used in the AKP mice has a series of *LoxP* cassettes flanking exon 8, leading to deletion of the protein.<sup>43</sup> Other *Arid1a*<sup>flox</sup> alleles have a series of *LoxP* cassettes flanking exons 5 to 6, leading to deletion of the ARID DNA-binding domain or point mutations in the ARID domain, which allow protein expression without DNA binding.<sup>14,52</sup> Regardless of the *Arid1a*<sup>flox</sup> allele used, conditional deletion of *Arid1a* in the uterus did not result in endometrial cancer.<sup>13–17</sup> Development of endometrial cancer with conditional deletion of *Arid1a* requires combination with deletion of *Pten* or expression of an oncogenic *Pik3ca*<sup>H1047R</sup> allele.<sup>13,14</sup> The additional genetic changes led to the development of cancer in mice with two different genetic backgrounds (ie, CD-1 or C57BL/6/129S1/BALB/c mix).<sup>13,14</sup> Using lactoferrin *Cre* to delete *Arid1a* and express mutant *PIK3CA* in the epithelial cells of the uterus, mice developed invasive endometrial adenocarcinoma at 14 to 17 weeks.<sup>14</sup> This development of endometrial cancer at older age is consistent with the potential for AKP mice to develop endometrial cancer. However, it was not observed because of early euthanasia due to vaginal tumors. A detailed description of each genetically engineered female reproductive tract *Arid1a* mouse model is provided in Supplemental Table S6.<sup>53</sup>

Mechanistically, the early development of aggressive and highly penetrant vaginal tumors may be in part due to the suppression of oncogene-induced cellular senescence mediated by ARID1A loss. Cellular senescence is frequently found in aging or cancerous tissue, potentially because of oncogenic signaling.<sup>54</sup> Oncogenic KRAS<sup>G12D</sup> expression in pancreatic cancer cell lines induces cellular senescence.<sup>55</sup> Of note, ARID1A knockdown repressed oncogene-induced cellular senescence in KRAS<sup>G12D</sup> pancreatic cell lines, leading to cell cycle progression.<sup>55</sup> Consistent with this view, ARID1A promoter hypermethylation and decreased ARID1A expression led to increased squamous cell carcinoma progression *in vitro* and *in vivo*.<sup>56</sup> Cyclin-dependent kinase inhibitor 2A or p16 is a potential marker of cellular senescence. Specifically, as expected, p16 staining was localized to the nucleus<sup>46,49</sup> in the *Pgr*<sup>+/+</sup> mouse. The AKP vaginal squamous cell carcinoma expressed p16 in both the nucleus and the cytoplasm (Figure 3). Cytoplasmic p16 staining may represent the cellular mechanism in which p16 becomes inactivated and allows for tumor progression.<sup>57,58</sup> Both the functional role of *Kras*-mediated oncogenic cellular senescence in vaginal squamous cell carcinoma development and the mechanistic role of *Arid1a* loss in the translocation of p16 warrant further investigation.

*Kras*<sup>G12D</sup>-induced vaginal papillomas have been reported in mice.<sup>29,59</sup> Spontaneous vaginal papillomas were noted when *Kras*<sup>G12D</sup> was expressed through the insulin promoter factor 1 *Cre* recombinase (*Ipf1*<sup>Cre</sup>, also known as *Pdx1*<sup>Cre</sup>) with a median age of 235 days.<sup>59</sup> When *Kras*<sup>G12D</sup> was expressed with the *Pgr*<sup>Cre</sup> (KP mice), vaginal papillomas



began as early as 2 months. However, KP mice did not exhibit malignant tumors.<sup>29</sup> AKP female mice exhibited malignant vaginal tumors earlier (Figure 2) than KP female mice which developed nonmalignant lesions.<sup>29</sup> The benign nature of KP and the *Ipf1<sup>Cre</sup>* models suggests that a secondary hit may be necessary for transformation to malignancy. This hypothesis is supported by the presence of vaginal squamous cell carcinoma in *Kras<sup>G12D</sup>* mice with a *Pten*-inactivating mutation driven by vaginally delivered adenovirus *Cre*.<sup>30</sup> The vaginal lesions are exophytic, protruding externally from the vagina, and histologically resemble those described in AKP mice.<sup>30</sup>

The effects of 17- $\beta$ -estradiol treatment on tumor growth were somewhat surprising. Clinically, vaginal squamous cell carcinoma is not treated as a hormone-responsive disease. Although 17- $\beta$ -estradiol is clinically used to increase epithelial cell thickness and treat the symptoms associated with postmenopausal vaginal atrophy, the mechanisms involved in squamous cell proliferation and differentiation are not well studied. Furthermore, the effects of 17- $\beta$ -estradiol treatment on progesterone receptor expression, and thus, the function of *Cre* recombinase in the vagina, warrant further study.

Clinically, 17,600 women were diagnosed with primary vaginal squamous cell carcinoma, and 8062 women died of vaginal squamous cell carcinoma worldwide in 2018.<sup>4</sup> The number of new cases of vaginal cancer in the United States for 2020 were 6230, with 1450 deaths.<sup>60</sup> Although vaginal cancer is not a common cancer, the incidence of vaginal squamous cell carcinoma disproportionately affects black women. The incidence of vaginal cancer is 72% higher in black women than white women, making vaginal cancer a disease of significant health disparity.<sup>61</sup> Because the HPV vaccine's impact decreases the prevalence of HPV-dependent squamous cell carcinoma, this model of HPV-negative squamous cell carcinoma becomes even more critical. Similar to vaginal, anal, vulvar, and cervical cancers, head and neck cancers are considered HPV-associated diseases. Survival of patients with HPV-positive head and neck cancers is significantly higher than that of those with HPV-negative tumors.<sup>62</sup> Mouse models with HPV-negative disease offer a significant opportunity to study these rarer tumors.

The genetically engineered mouse model that targets the knockout of the tumor suppressor *Arid1a* and the knock-in of oncogenic *Kras<sup>G12D</sup>* in the gynecologic tract leads to primary squamous cell carcinoma of the vagina. With age, the AKP mice develop preneoplastic lesions and eventually invasive squamous cell carcinoma. The role of hormone expression in primary squamous cell carcinoma of the vagina alludes to the potential mechanistic and therapeutic targets. Finally, we speculate the possible mechanism for tumor progression of repressed oncogene-induced cellular senescence via translocation of p16 from the nucleus to the cytoplasm. This genetically engineered mouse model of primary squamous cell carcinoma of the vagina may lead to

advances in early detection, understanding of initiation and progression, and novel treatment options.

## Author Contributions

X.W., M.P., and S.M.H. designed the study, collected and analyzed data, performed literature search, and generated figures. J.R.H.W. interpreted data, performed literature search, and generated figures. R.E.E. analyzed data, performed literature search, and generated figures. J.P.L. and F.J.D. contributed new reagents/analytic tools. All authors wrote the paper and approved the submitted and published versions. All authors agree to be accountable for all aspects of the work in ensuring that questions related to the accuracy or integrity of any part of the work are appropriately investigated or resolved. S.M.H. is the guarantor of this work, and as such, had full access to all the data in the study and takes responsibility for the integrity of the data and the accuracy of the data analysis.

## Acknowledgments

We thank Julio Agno for technical support, Dr. Joanne S. Richards for the *Kras<sup>Lox-Stop-Lox-G12D/+</sup>* mice, and Dr. Zhong Wang for the *Arid1a<sup>flox/flox</sup>* mice.

## Supplemental Data

Supplemental material for this article can be found at <http://doi.org/10.1016/j.ajpath.2021.03.013>.

## References

- Zehir A, Benayed R, Shah RH, Syed A, Middha S, Kim HR, et al: Mutational landscape of metastatic cancer revealed from prospective clinical sequencing of 10,000 patients. *Nat Med* 2017, 23: 703–713
- Hoadley KA, Yau C, Hinoue T, Wolf DM, Lazar AJ, Drill E, Shen R, Taylor AM, Cherniack AD, Thorsson V, Akbani R, Bowlby R, Wong CK, Wiznerowicz M, Sanchez-Vega F, Robertson AG, Schneider BG, Lawrence MS, Noushmehr H, Malta TM, Cancer Genome Atlas N, Stuart JM, Benz CC, Laird PW: Cell-of-Origin Patterns Dominate the Molecular Classification of 10,000 Tumors from 33 Types of Cancer. *Cell* 2018, 173:291–304 e6
- Sung H, Ferlay J, Siegel RL, Laversanne M, Soerjomataram I, Jemal A, Bray F: Global cancer statistics 2020: GLOBOCAN estimates of incidence and mortality worldwide for 36 cancers in 185 countries. *CA Cancer J Clin* 2021, 71:209–249
- Bray F, Ferlay J, Soerjomataram I, Siegel RL, Torre LA, Jemal A: Global cancer statistics 2018: GLOBOCAN estimates of incidence and mortality worldwide for 36 cancers in 185 countries. *CA Cancer J Clin* 2018, 68:394–424
- Chava S, Gupta R: Identification of the mutational landscape of gynecological malignancies. *J Cancer* 2020, 11:4870–4883
- Wiegand KC, Shah SP, Al-Agha OM, Zhao Y, Tse K, Zeng T, et al: ARID1A mutations in endometriosis-associated ovarian carcinomas. *N Engl J Med* 2010, 363:1532–1543
- Jones S, Wang TL, Shih IeM, Mao TL, Nakayama K, Roden R, Glas R, Slamon D, Diaz LA Jr, Vogelstein B, Kinzler KW,

- Velculescu VE, Papadopoulos N: Frequent mutations of chromatin remodeling gene ARID1A in ovarian clear cell carcinoma. *Science* 2010, 330:228–231
8. Cancer Genome Atlas Research N, Kandoth C, Schultz N, Cherniack AD, Akbani R, Liu Y, Shen H, Robertson AG, Pashtan I, Shen R, Benz CC, Yau C, Laird PW, Ding L, Zhang W, Mills GB, Kucherlapati R, Mardis ER, Levine DA: Integrated genomic characterization of endometrial carcinoma. *Nature* 2013, 497:67–73
  9. Guan B, Mao TL, Panuganti PK, Kuhn E, Kurman RJ, Maeda D, Chen E, Jeng YM, Wang TL, Shih IeM: Mutation and loss of expression of ARID1A in uterine low-grade endometrioid carcinoma. *Am J Surg Pathol* 2011, 35:625–632
  10. Guan B, Wang TL, Shih IeM: ARID1A, a factor that promotes formation of SWI/SNF-mediated chromatin remodeling, is a tumor suppressor in gynecologic cancers. *Cancer Res* 2011, 71:6718–6727
  11. Jones S, Li M, Parsons DW, Zhang X, Wesselung J, Kristel P, Schmidt MK, Markowitz S, Yan H, Bigner D, Hruban RH, Eshleman JR, Iacobuzio-Donahue CA, Goggins M, Maitra A, Malek SN, Powell S, Vogelstein B, Kinzler KW, Velculescu VE, Papadopoulos N: Somatic mutations in the chromatin remodeling gene ARID1A occur in several tumor types. *Hum Mutat* 2012, 33:100–103
  12. Cancer Genome Atlas Research Network; Albert Einstein College of Medicine; Analytical Biological Services; Barretos Cancer Hospital; Baylor College of Medicine; Beckman Research Institute of City of Hope; Buck Institute for Research on Aging; Canada's Michael Smith Genome Sciences Centre; Harvard Medical School; Helen F. Graham Cancer Center & Research Institute at Christiana Care Health Services; HudsonAlpha Institute for Biotechnology; ILSbio, LLC; Indiana University School of Medicine; Institute of Human Virology; Institute for Systems Biology; International Genomics Consortium; Leidos Biomedical; Massachusetts General Hospital; McDonnell Genome Institute at Washington University; Medical College of Wisconsin; Medical University of South Carolina; Memorial Sloan Kettering Cancer Center; Montefiore Medical Center; NantOmics; National Cancer Institute; National Hospital, Abuja, Nigeria; National Human Genome Research Institute; National Institute of Environmental Health Sciences; National Institute on Deafness & Other Communication Disorders; Ontario Tumour Bank, London Health Sciences Centre; Ontario Tumour Bank, Ontario Institute for Cancer Research; Ontario Tumour Bank, The Ottawa Hospital; Oregon Health & Science University; Samuel Oschin Comprehensive Cancer Institute, Cedars-Sinai Medical Center; SRA International; St Joseph's Candler Health System, et al: Integrated genomic and molecular characterization of cervical cancer. *Nature* 2017, 543:378–384
  13. Suryo Rahmanto Y, Shen W, Shi X, Chen X, Yu Y, Yu ZC, Miyamoto T, Lee MH, Singh V, Asaka R, Shimberg G, Vitolo MI, Martin SS, Wirtz D, Drapkin R, Xuan J, Wang TL, Shih IM: Inactivation of Arid1a in the endometrium is associated with endometrioid tumorigenesis through transcriptional reprogramming. *Nat Commun* 2020, 11:2717
  14. Wilson MR, Reske JJ, Holladay J, Wilber GE, Rhodes M, Koeman J, Adams M, Johnson B, Su RW, Joshi NR, Patterson AL, Shen H, Leach RE, Teixeira JM, Fazleabas AT, Chandler RL: ARID1A and PI3-kinase pathway mutations in the endometrium drive epithelial transdifferentiation and collective invasion. *Nat Commun* 2019, 10:3554
  15. Wang X, Khatri S, Broaddus R, Wang Z, Hawkins SM: Deletion of Arid1a in reproductive tract mesenchymal cells reduces fertility in female mice. *Biol Reprod* 2016, 94:93
  16. Kim TH, Yoo JY, Wang Z, Lydon JP, Khatri S, Hawkins SM, Leach RE, Fazleabas AT, Young SL, Lessey BA, Ku BJ, Jeong JW: ARID1A is essential for endometrial function during early pregnancy. *PLoS Genet* 2015, 11:e1005537
  17. Marquardt RM, Kim TH, Yoo JY, Teasley HE, Fazleabas AT, Young SL, Lessey BA, Arora R, Jeong JW: Endometrial epithelial ARID1A is critical for uterine gland function in early pregnancy establishment. *FASEB J* 2021, 35:e21209
  18. Guan B, Rahmanto YS, Wu RC, Wang Y, Wang Z, Wang TL, Shih IeM: Roles of deletion of Arid1a, a tumor suppressor, in mouse ovarian tumorigenesis. *J Natl Cancer Inst* 2014, 106
  19. Wendel JRH, Wang X, Hawkins SM: The endometriotic tumor microenvironment in ovarian cancer. *Cancers (Basel)* 2018, 10:E261
  20. Bitler BG, Wu S, Park PH, Hai Y, Aird KM, Wang Y, Zhai Y, Kossenkov AV, Vara-Ailor A, Rauscher FJ III, Zou W, Speicher DW, Huntsman DG, Conejo-Garcia JR, Cho KR, Christianson DW, Zhang R: ARID1A-mutated ovarian cancers depend on HDAC6 activity. *Nat Cell Biol* 2017, 19:962–973
  21. Chandler RL, Damrauer JS, Raab JR, Schisler JC, Wilkerson MD, Didion JP, Starmer J, Serber D, Yee D, Xiong J, Darr DB, Pardo-Manuel de Villena F, Kim WY, Magnuson T: Coexistent ARID1A-PIK3CA mutations promote ovarian clear-cell tumorigenesis through pro-tumorigenic inflammatory cytokine signalling. *Nat Commun* 2015, 6:6118
  22. Zhai Y, Kuick R, Tipton C, Wu R, Sessine M, Wang Z, Baker SJ, Fearon ER, Cho KR: Arid1a inactivation in an Apc- and Pten-defective mouse ovarian cancer model enhances epithelial differentiation and prolongs survival. *The J Pathology* 2016, 238:21–30
  23. Engelsen IB, Akslen LA, Salvesen HB: Biologic markers in endometrial cancer treatment. *APMIS* 2009, 117:693–707
  24. Dobrzycka B, Terlikowski SJ, Mazurek A, Kowalczyk O, Niklinska W, Chyczewski L, Kulikowski M: Mutations of the KRAS oncogene in endometrial hyperplasia and carcinoma. *Folia Histochem Cytobiol* 2009, 47:65–68
  25. Kandoth C, McLellan MD, Vandin F, Ye K, Niu B, Lu C, Xie M, Zhang Q, McMichael JF, Wyczalkowski MA, Leiserson MDM, Miller CA, Welch JS, Walter MJ, Wendl MC, Ley TJ, Wilson RK, Raphael BJ, Ding L: Mutational landscape and significance across 12 major cancer types. *Nature* 2013, 502:333–339
  26. Fan HY, Liu Z, Paquet M, Wang J, Lydon JP, DeMayo FJ, Richards JS: Cell type-specific targeted mutations of Kras and Pten document proliferation arrest in granulosa cells versus oncogenic insult to ovarian surface epithelial cells. *Cancer Res* 2009, 69:6463–6472
  27. Mullany LK, Fan HY, Liu Z, White LD, Marshall A, Gunaratne P, Anderson ML, Creighton CJ, Xin L, Deavers M, Wong KK, Richards JS: Molecular and functional characteristics of ovarian surface epithelial cells transformed by KrasG12D and loss of Pten in a mouse model in vivo. *Oncogene* 2011, 30:3522–3536
  28. Dinulescu DM, Ince TA, Quade BJ, Shafer SA, Crowley D, Jacks T: Role of K-ras and Pten in the development of mouse models of endometriosis and endometrioid ovarian cancer. *Nat Med* 2005, 11:63–70
  29. Kim TH, Wang J, Lee KY, Franco HL, Broaddus RR, Lydon JP, Jeong JW, Demayo FJ: The synergistic effect of conditional Pten loss and oncogenic K-ras mutation on endometrial cancer development occurs via decreased progesterone receptor action. *J Oncol* 2010, 2010:139087
  30. Blum JS, Weller CE, Booth CJ, Babar IA, Liang X, Slack FJ, Saltzman WM: Prevention of K-Ras- and Pten-mediated intravaginal tumors by treatment with camptothecin-loaded PLGA nanoparticles. *Drug Deliv Transl Res* 2011, 1:383–394
  31. Kun EHS, Tsang YTM, Lin S, Pan S, Medapalli T, Malpica A, Richards JS, Gershenson DM, Wong KK: Differences in gynecologic tumor development in Amhr2-Cre mice with KRAS(G12D) or KRAS(G12V) mutations. *Sci Rep* 2020, 10:20678
  32. Fan HY, Shimada M, Liu Z, Cahill N, Noma N, Wu Y, Gossen J, Richards JS: Selective expression of KrasG12D in granulosa cells of the mouse ovary causes defects in follicle development and ovulation. *Development* 2008, 135:2127–2137
  33. Tirodkar TS, Budi RA, Elishaev E, Zhang L, Mony JT, Brozick J, Edwards RP, Vlad AM: MUC1 positive, Kras and Pten driven mouse gynecologic tumors replicate human tumors and vary in survival and nuclear grade based on anatomical location. *PLoS One* 2014, 9:e102409



34. Budiu RA, Diaconu I, Chrissluis R, Dricu A, Edwards RP, Vlad AM: A conditional mouse model for human MUC1-positive endometriosis shows the presence of anti-MUC1 antibodies and Foxp3+ regulatory T cells. *Dis Model Mech* 2009, 2:593–603
35. Tang FH, Hsieh TH, Hsu CY, Lin HY, Long CY, Cheng KH, Tsai EM: KRAS mutation coupled with p53 loss is sufficient to induce ovarian carcinosarcomas in mice. *Int J Cancer* 2017, 140:1860–1869
36. Mirkovic J, McFarland M, Garcia E, Sholl LM, Lindeman N, MacConaill L, Dong F, Hirsch M, Nucci MR, Quick CM, Crum CP, McCluggage WG, Howitt BE: Targeted genomic profiling reveals recurrent KRAS mutations in mesonephric-like adenocarcinomas of the female genital tract. *Am J Surg Pathol* 2018, 42:227–233
37. Ishikawa M, Nakayama K, Nakamura K, Ono R, Sanuki K, Yamashita H, Ishibashi T, Minamoto T, Iida K, Razia S, Ishikawa N, Kyo S: Affinity-purified DNA-based mutation profiles of endometriosis-related ovarian neoplasms in Japanese patients. *Oncotarget* 2018, 9:14754–14763
38. Hollis RL, Thomson JP, Stanley B, Churchman M, Meynert AM, Rye T, Bartos C, Iida Y, Croy I, Mackean M, Nussey F, Okamoto A, Semple CA, Gourley C, Herrington CS: Molecular stratification of endometrioid ovarian carcinoma predicts clinical outcome. *Nat Commun* 2020, 11:4995
39. Committee for the Update of the Guide for the Care and Use of Laboratory Animals; National Research Council: *Guide for the Care and Use of Laboratory Animals*. Eighth Edition. Washington, DC, National Academies Press, 2011
40. Soyal SM, Mukherjee A, Lee KY, Li J, Li H, DeMayo FJ, Lydon JP: Cre-mediated recombination in cell lineages that express the progesterone receptor. *Genesis* 2005, 41:58–66
41. Hadji A, Ceppi P, Murmann AE, Brockway S, Pattanayak A, Bhinder B, Hau A, De Chant S, Parimi V, Kolesza P, Richards J, Chandel N, Djaballah H, Peter ME: Death induced by CD95 or CD95 ligand elimination. *Cell Rep* 2014, 7:208–222
42. Wang X, Wendel JRH, Emerson RE, Broadus RR, Creighton CJ, Rusch DB, Buechlein A, DeMayo FJ, Lydon JP, Hawkins SM: Pten and Dicer1 loss in the mouse uterus causes poorly differentiated endometrial adenocarcinoma. *Oncogene* 2020, 39:6286–6299
43. Gao X, Tate P, Hu P, Tjian R, Skarnes WC, Wang Z: ES cell pluripotency and germ-layer formation require the SWI/SNF chromatin remodeling component BAF250a. *Proc Natl Acad Sci U S A* 2008, 105:6656–6661
44. Johnson L, Mercer K, Greenbaum D, Bronson RT, Crowley D, Tuveson DA, Jacks T: Somatic activation of the K-ras oncogene causes early onset lung cancer in mice. *Nature* 2001, 410:1111–1116
45. Darragh TM, Colgan TJ, Thomas Cox J, Heller DS, Henry MR, Luff RD, McCalmont T, Nayar R, Palefsky JM, Stoler MH, Wilkinson EJ, Zaino RJ, Wilbur DC: Members of the Last Project Work Group. The Lower Anogenital Squamous Terminology Standardization project for HPV-associated lesions: background and consensus recommendations from the College of American Pathologists and the American Society for Colposcopy and Cervical Pathology. *Int J Gynecol Pathol* 2013, 32:76–115
46. Malpica A. Neoplastic Lesions of the Vagina. *Gynecologic Pathology: A Volume in Foundations in Diagnostic Pathology Series*. Edited by Nucci MR, Parra-Herran C. ed 2. Philadelphia, PA: Elsevier, 2020. pp. 153–184. 19103-2899
47. Moll R, Divo M, Langbein L: The human keratins: biology and pathology. *Histochem Cell Biol* 2008, 129:705–733
48. Kurita T, Cunha GR, Robboy SJ, Mills AA, Medina RT: Differential expression of p63 isoforms in female reproductive organs. *Mech Dev* 2005, 122:1043–1055
49. Bertoli HK, Rasmussen CL, Sand FL, Albieri V, Norrild B, Verdoort F, Kjaer SK: Human papillomavirus and p16 in squamous cell carcinoma and intraepithelial neoplasia of the vagina. *Int J Cancer* 2019, 145:78–86
50. Ceccarelli S, D'Amici S, Vescarelli E, Coluccio P, Matricardi P, di Gioia C, Benedetti Panici P, Romano F, Frati L, Angeloni A, Marchese C: Topical KGF treatment as a therapeutic strategy for vaginal atrophy in a model of ovariectomized mice. *J Cellular Molecular Medicine* 2014, 18:1895–1907
51. Pandita P, Wang X, Jones DE, Collins K, Hawkins SM: Unique molecular features in high-risk histology endometrial cancers. *Cancers (Basel)* 2019, 11:1665
52. Chandler RL, Brennan J, Schisler JC, Serber D, Patterson C, Magnuson T: ARID1a-DNA interactions are required for promoter occupancy by SWI/SNF. *Mol Cell Biol* 2013, 33:265–280
53. Wilson MR, Holladay J, Chandler RL: A mouse model of endometriosis mimicking the natural spread of invasive endometrium. *Hum Reprod* 2020, 35:58–69
54. Campisi J, d'Adda di Fagagna F: Cellular senescence: when bad things happen to good cells. *Nat Rev Mol Cell Biol* 2007, 8:729–740
55. Li ZY, Zhu SS, Chen XJ, Zhu J, Chen Q, Zhang YQ, Zhang CL, Guo TT, Zhang LM: ARID1A suppresses malignant transformation of human pancreatic cells via mediating senescence-associated miR-503/CDKN2A regulatory axis. *Biochem Biophys Res Commun* 2017, 493:1018–1025
56. Luo Q, Wu X, Chang W, Zhao P, Zhu X, Chen H, Nan Y, Luo A, Zhou X, Su D, Jiao W, Liu Z: ARID1A hypermethylation disrupts transcriptional homeostasis to promote squamous cell carcinoma progression. *Cancer Res* 2020, 80:406–417
57. Evangelou K, Bramis J, Peros I, Zacharatos P, Dasiou-Plakida D, Kalogeropoulos N, Asimacopoulos PJ, Kittas C, Marinos E, Gorgoulis VG: Electron microscopy evidence that cytoplasmic localization of the p16(INK4A) "nuclear" cyclin-dependent kinase inhibitor (CKI) in tumor cells is specific and not an artifact: a study in non-small cell lung carcinomas. *Biotech Histochem* 2004, 79:5–10
58. Nilsson K, Landberg G: Subcellular localization, modification and protein complex formation of the cdk-inhibitor p16 in Rb-functional and Rb-inactivated tumor cells. *Int J Cancer* 2006, 118:1120–1125
59. Gades NM, Ohashi A, Mills LD, Rowley MA, Predmore KS, Marler RJ, Couch FJ: Spontaneous vulvar papillomas in a colony of mice used for pancreatic cancer research. *Comp Med* 2008, 58:271–275
60. Siegel RL, Miller KD, Jemal A: Cancer statistics, 2020. *CA Cancer J Clin* 2020, 70:7–30
61. Gadducci A, Fabrini MG, Lanfredini N, Sergiampietri C: Squamous cell carcinoma of the vagina: natural history, treatment modalities and prognostic factors. *Crit Rev Oncol Hematol* 2015, 93:211–224
62. Mahal BA, Catalano PJ, Haddad RI, Hanna GJ, Kass JI, Schoenfeld JD, Tishler RB, Margalit DN: Incidence and demographic burden of HPV-associated oropharyngeal head and neck cancers in the United States. *Cancer Epidemiol Biomarkers Prev* 2019, 28:1660–1667